A Critical Review of Age Treatment Hardening Mechanisms in Aluminum Alloys

Víctor M. Alcántara Alza[1]

[1](Mechanics and Energy, Faculty of Engineering/ National university of Trujillo, Perú)

Abstract:

Aluminum alloys are used in various sectors of the industry, due to their excellent combination strength and ductility, high strength/ weight ratio, corrosion resistance, fatigue resistance, and high fracture toughness, among others. But not all aluminum alloys present this set of properties simultaneously. The desired properties in service conditions are achieved through many factors, such as the chemical composition, the manufacturing method, plastic deformation and, above all, the thermal treatments, which allow strong precipitation hardening.Butit should be noted that the so-called "aging" heat treatments are only applicable to certain series of aluminum alloys, such as: 2xxx, 6xxx, 7000xxx and 9xxx.When the precipitation hardening treatment is applied, the precipitated particles must be coherent and coplanar with the matrix.On the other hand, to achieve precipitation hardening at high temperatures of aluminum alloys, it is necessary the hardening phases (precipitates) must be thermodynamically stable and resist coursing, at temperature of interest.Precipitation hardening is achieved by precipitation sequences, which are very complex and include several metastable phases. It can also be said the way in which these phases nucleate in the presence of the preceding phase is complex.The beginning of each sequence implies the presence of GP and GPB regions. The first is common to almost all precipitation sequences. The GPB zone appears only in certain sequences, and in some of them, gives rise the formation of the GPB2 zone.Still exists controversybetween researchers, regarding the stoichiometry and requirements for the formation of the GPB and GPB2 zones.Despite numerous research papers; the precipitation behavior of certain aluminum alloys remains poorly understood, and the same thing is happening of many precipitated phases that are not yet well defined.The objective of this study focuses on reviewing the hardening mechanisms that allow increasing the hardness and mechanical resistance of these aluminum alloys and recommending the appropriate parameters so that the aging treatment leads to a sequence, where there are no harmful phases or precipitates within the aged aluminum.

Key Word*: Aluminium alloys, Aging treatment, Precipitation behavior, Coherent precipitates, GP zones*

I. Introduction

Aluminum alloys have great advantages: a high specific modulus, good specific strength, higher corrosion resistance and better workability. Due to this superior combination of properties compared to other alloys; They are now widely applied in a number of industries, in aerospace, automotive, high-speed rail engineering and so on. In recent decades, almost all advanced industrial countries have carried out projects to plan, guide and support research and development of aluminum alloys[1 - 3].

The strength and hardness of some metal alloys can be increased by the formation of extremely small, uniformly dispersed particles of a second phase within the matrix, which result from submit the part to a cycle of heat treatment known as precipitation hardening or aged, because it develops over time [4-9].In aluminum alloys, to improve their performance, these hardening phases (precipitates) must be thermodynamically stable and resist the thickened at the temperature of interest. This is obtained if the hardening precipitates are coherent and coplanar with the matrix, with which microstructural stability is achieved[10]. The resistance of aluminum alloys is due to the fact that the impurity atoms in solution produce a deformation of the dislocation network and of the impurity atoms, blocking the movement of these dislocations, thus greater hardness and mechanical resistance isachieved[11].

For an alloy to be harden by precipitation, it must meet certain requirements: 1) That the phase diagram has partial solubility; 2) That the maximum solubility of one component in another is considerable; 3) That the solubility decreases with the decrease in temperature [12].

Not all aluminum alloys respond to "precipitation hardening" heat treatment. Those that can be strengthened or hardened by precipitation are called "heat treatable aluminum alloys". When aluminum alloys of this class are heated to a high temperature (solid solution temperature) and kept there for a sufficient period of

---

time, the alloying elements dissolve in the matrix in high concentration.When the alloy is rapidly cooled to low temperature, the alloying

element atoms can "freeze" in the Al matrix to form a supersaturated solid solution (SSSS). When this SSSS is heated to moderate temperature, the supersaturated alloying elements separate and combine with other elements to form intermetallic compound particles in the Al matrix; this is called precipitation. Alloying elements frequently used to generate precipitates in aluminum alloys include Cu, Zn, Mg, Si, and Li.

When the aging treatment is applied; it is usual to seek to maximize the amount solutes that participate in the precipitation process. In this regard, a commonly used aging cycle for aluminum alloys is T4 (natural aging) and T6 (artificial aging). In both cases, the alloy is first dissolved, and then rapidly cooled (quenching) and aged in air (T4) or by bringing it to a suitable elevated temperature (~ 150°C) for a specified time (T6). Recent results have shown that mechanical properties, such as creep and fatigue strength, are improved with aging, and can be further improved by deliberately encouraging solute elements to partition homogeneously in the solid solution. Matrix together with the fine precipitates, which are the ones that promote the strengthening. **[13, 14].**

The main alloying elements of aluminum are: copper, magnesium, zinc and manganese. In smaller quantities, as impurities or additives: iron, silicon, chromium and titanium. For special alloys, nickel, cobalt, silver, lithium, vanadium, zirconium, tin, lead, cadmium and bismuth are added **[15].**Heat treatable aluminum alloys can be classified according to the naming convention established by Alcoa, in series of the type: 2000, 6000 series, 7000 series and 9000 series respectively.

It has often been believed that an alloy that has been aged at a high temperature, its mechanical properties remain stable during exposure for an indefinite time, at a significantly lower temperature; However, Loeffler et al. **[16],**revealed that highly saturated Al-Zn alloys initially aged at 180 °C continued to harden by so-called "secondary precipitation" when cooled and kept at room temperature. Similar behavior has since been observed for highly saturated lithium-containing alloys aged first at 170 °C and then exposed for long periods at 60–130 °C.**[17].** In this case, the strength and hardness increase with time, but the alloys tend to become brittle. When different alloying elements are used, the precipitates are different. The basic necessary condition of these precipitates, even if they have different morphology and structures, is to be effective in restricting the movement of dislocations, both at room temperature and high temperatures [18].

The fundamental stage of aging process consists in acceleration of phenomenon of decomposition of supersaturated solid solution (SSSS), which results in the precipitation of coarse intermetallic particles [19-21];which are later refined with natural or artificial aging.

There are many studies regarding the phenomenon of precipitation in aluminum alloys. Some of them will be mentioned. Regarding the AA7075 alloy, determined that the precipitation of second phases occurs from the SSSS solid solution and that the number and size of these phases increase with the decrease in temperature of the quenching medium**[22].** The kinetic parameters of the alloy AA 7A09; can be obtained from the analysis of the precipitation results, showing that for this alloy, the precipitation of the η phase is a diffusional transformation that can be described by the Avram equation: $f = 1 - \exp(-kt^n)$**[23].**Dolan and Robinson**[24]**investigated the behavior of three alloys AA 7175-T73, AA 6061-T6 and AA 2017A-T4, by immersion and spray quenching using cold water. As a result, they generated time-temperature-property (TTP) curves for each alloy. These curves were generated in the critical temperature range, where precipitation occurs more quickly, and they found a very good relationship between the hardness measured and that predicted in the curves.They concluded that although rapid cooling guarantees good mechanical properties, thermal gradients can be large enough to produce high levels of residual stresses. Reducing cooling rates during quenching can reduce the magnitude of residual stresses, however, it can also be detrimental to mechanical properties, particularly for quench-sensitive aluminum alloys.

The aim of this paper is to make a critical review of the mechanisms of precipitation hardening (aging) in aluminum alloys treatable by this procedure, without taking into account any intermediate process of plastic deformation. The most focused topic is about sequences of precipitates of each alloy series that is treatable by aging.To date have been described many particulars cases, but the phenomenon itself is notfully understood; even generating interpretation controversies among researchers.

II. General Overview

2.1. Phase Transformation by Precipitation.

When a supersaturated SSSS solid solution is aged at a temperature within a biphasic field, particles of the new phase appear in the matrix which increase in size with aging time. After the formation of the new phase; the individual particles continue to grow with the solute atoms around them, because the solute atoms grow and the degree of supersaturation decreases. The solute concentration in the matrix decreases until it reaches the

equilibrium concentration, that is, it reaches the solubility limit which corresponds to the maximum soluble concentration of the matrix. Then, the formation of the new phase is said to be complete and its volume fraction remains constant. **[25-27].**Figure 1(a) shows a solvus curve of phase α that decreases with temperature. Considering an alloy of composition Xm. This alloy is solubilized at a temperature Tq obtaining a homogeneous phase. If this solubilized alloy is rapidly cooled from Tq to Ta, it is possible to retain the high temperature phase in a supersaturated state. Keeping the alloy at Ta, it decomposes into a mixture of "α" of composition Xm and "β" of composition Xe. In this way the nucleus of the phase β appears and grows by absorption of solute from the matrix. Thus, the solute content of the matrix is depleted from Xm to Xe. This phase transformation is known as precipitation.**[28],** and is described by the equation:$\alpha(Xm) \rightarrow \alpha(Xe) + \beta(X\beta)$ (1)

2.2. The Process Evolution and Precipitates.

With aging, the alloys harden and strengthen due to the precipitation of intermediate phases that depend on the process parameters, (especially: time and temperature), which leads to a condition of maximum aging or peak aging, where the properties mechanics reach a maximum value; but if the aging continues, a condition of excessive growth (overaging) is reached, where the mechanical properties decrease. Figure 1(b) shows the evolution of the hardness and mechanical resistance of an aluminum alloy throughout the aging process**[29, 30].**If the overaging is carried out at a higher temperature, or for a longer time than that required to reach maximum aging (i.e., that required for the critical dispersion of particles), what causes is an agglomeration of precipitated particles, giving rise to a loss of hardness and resistance, as indicated in graph 1(b).
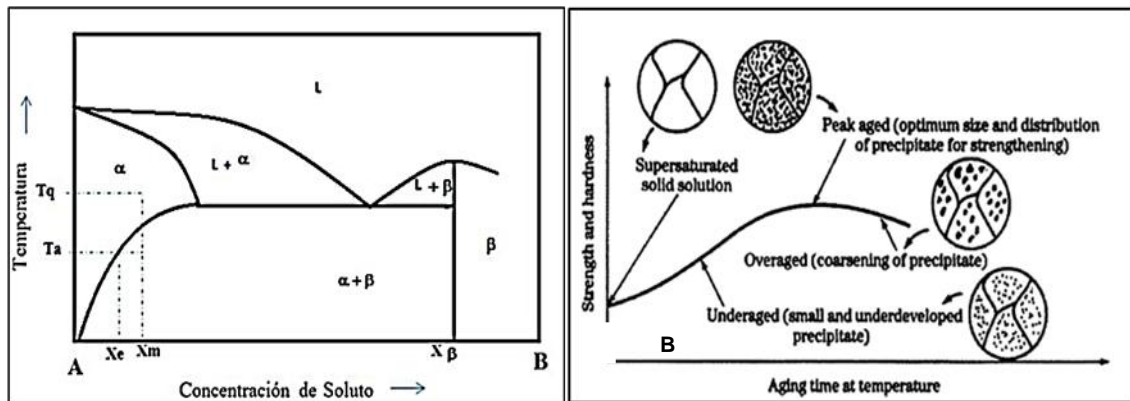
Figure 1. (A)Schematic phase diagram of the precipitation reaction **[31]** (B) Evolution of the hardness and mechanical strength as a function of time and temperature treatment **[29, 30].**

2.3. Types and Characteristics of Precipitates in the Aged.

In age hardening, the properties of the alloy depend directly on the precipitates formed throughout the grain. Thus, for example, it has been found that approximately 10^{16} of these precipitates can be present in each cm3 of an Al-Cu-Mg-Ag alloy **[32].** Depending on the elastic mismatch and the interfacial energy, the precipitates can take different forms. For example, going from low interfacial energy and elastic deformation (coherence) to high interfacial energy and large mismatch (incoherence), the shape of the precipitate progresses through the following morphologies: cubic, disc, and needle **[33].** Table 1 shows the typical precipitates of aluminum alloys that are age hardening and Figure 2 shows a schematic representation of the stages of formation of these precipitates in an Al-Cu alloy.

Table 1. Precipitates that form in aluminum alloys according to the series that are heat treatable by aging.

Series	Master alloying elements	Precipitates
2000	Al, Cu, (Mg)	GP $\rightarrow \theta' \rightarrow \theta'$ (CuAl$_2$)
6000	Al, Mg, Si	GP $\rightarrow \beta' \rightarrow \beta''$ (Mg$_2$Si)
7000	Al, Zn, Mg	GP $\rightarrow \eta' \rightarrow \eta$ (MgZn$_2$)
9000	Al, Li	δ' (Al$_3$Li) $\rightarrow \delta$ (AlLi)
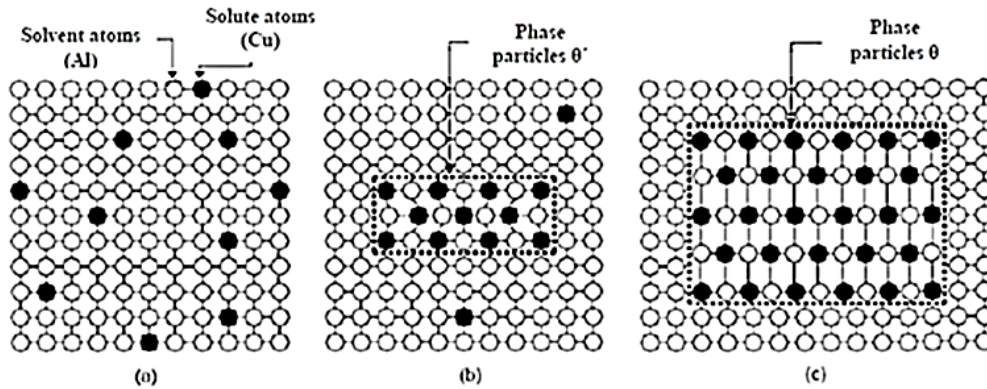
Figure 2. Schematic representation of the stages of equilibrium (θ) phase precipitate formation. (a) Supersaturated α solid solution, (b) Precipitated transition phase (θ´´), (c) Equilibrium phase (θ)**[34].**

2.4. Requirements for Precipitation Hardening.

❖ The basic requirement for precipitation hardening of an alloy system is to decrease the solubility limit (solvus line) with decreasing temperature **[35].**

❖ **The metastability** of the supersaturated phase after quenching is the necessary condition for it to be hardened in the subsequent aging process. This hypothesis is true, as long as the size and shape of the precipitated particles maintain continuity with the crystalline structure and are also consistent with it. Coherence is the concept that involves the continuity of the crystalline planes of the alloy matrix, even harboring a nucleus of the phase precipitated by supersaturation. If the discontinuity of the crystalline planes occurs in the environment of a precipitated particle that is incoherent, the precipitate will behave as a subgrain within the monocrystal and its action will be as if it were an inclusion defect.

❖ **A coherent precipitate** is a precipitate whose crystal structure and atomic arrangement have a continuous relationship with the matrix from which it was formed. The coherent precipitate provides excellent disruption of the atomic arrangement in the matrix and excellent hardening. Therefore**;** *Precipitation hardening is produced by the effect of precipitated particles that coherently deform the crystalline planes of the matrix in their surroundings.*(See Fig. 3).On the other hand, the characteristic that determines whether a precipitated phase is coherent or not is the coincidence or the degree of deregistration between the atomic spaces in the matrix lattice and in the precipitate lattice.**[36]** To achieve hardening at high temperatures of an aluminum alloy, it is necessary that the hardening phases (precipitates) must be thermodynamically stable and resist thickening at the temperature of interest. This is obtained if the hardening precipitates are coherent and coplanar with the matrix **[37].** This correspondence implies that the matrix-precipitate interface has a low energy with little tendency to thicken or coalesce.
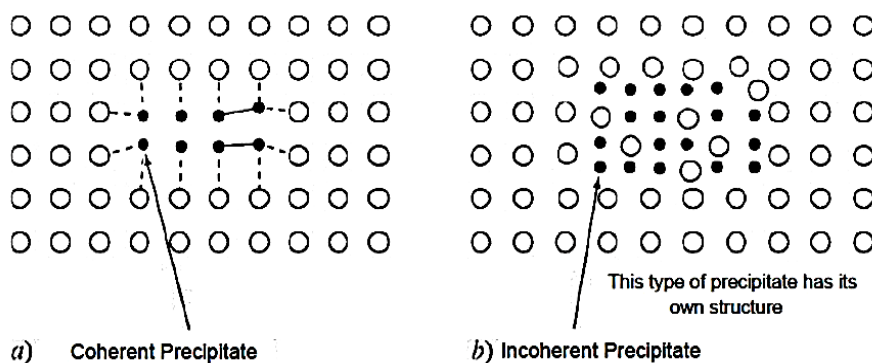
Figure3. Precipitated particle. a) Coherent. b) Incoherent with the crystal structure of the matrix. The coherent precipitate is associated with high strain energy and low surface energy, while the incoherent precipitate is associated with low strain energy and high surface energy..

2.5. Mechanisms of Hardening in the Aged

Current research directs its studies to the atomic mechanisms that control the formation of precipitates, so that, due to their size, shape and structure, they are effective in the restriction movement of dislocations at room temperature and at high temperatures [11]. The type of hardening depends on the type of precipitate, taking into account the size, shape, chemical composition and coherence, characteristics that change drastically with aging time. For very strong impenetrable precipitates, the most common mechanism is the so-called Orowan mechanism, which is outlined in Figure 4(A). Strong deviations are observed in the dislocation lines that stop their movement and hardening occurs. The obstacle is strong enough for the dislocation to tilt completely around it. The parts of the dislocation line contract until in (b) the dislocation has passed the obstacles leaving dislocation loops around the particle [38].

It is worth mentioning the Frank-Read mechanism; which is justified as the cause of the hardening, due to the greater difficulty imposed by the precipitates on the movement of the dislocations in the internal matrix phase. For this case of precipitation, the impediment of the movement of the dislocations can only be caused by the coherent precipitated particles. In Figure 4A line (a). indicates the interaction that a precipitate alignment can have with a dislocation line. The existence of the precipitate coherent with its stress field around the particle forces the dislocation to bend (lines b and c), with successive inflections. The strong bending of the dislocation can go as far as joining the ends around the dislocation, as seen in (d), until its cancellation, leaving a dislocation ring around the particle.

It is evident that the dislocation has required an increase in shear stress, τ, to cross the precipitate line. And that the slip resistance is increased by the interaction of the dislocation rings that surround the particles. This is the Frank-Read mechanism of particle bond hardening.

It Has been shown by dislocation theory that the increase in shear stress $\Delta\tau$ to cross the row of separated precipitates d and volumetric fraction f, fulfills the relationship given in equation (2).

$$\Delta\tau = K_{1g} f^{1/2} /r. \ln K_{L} r/f^{1/2} \tag{2}$$

Where: K1g and Kl are characteristic constants of the crystal.

Therefore: The coherent precipitate increases the shear stress required for sliding dislocations, traverse the rings justified by Frank-Read, according equation (2).

(A)	(B)
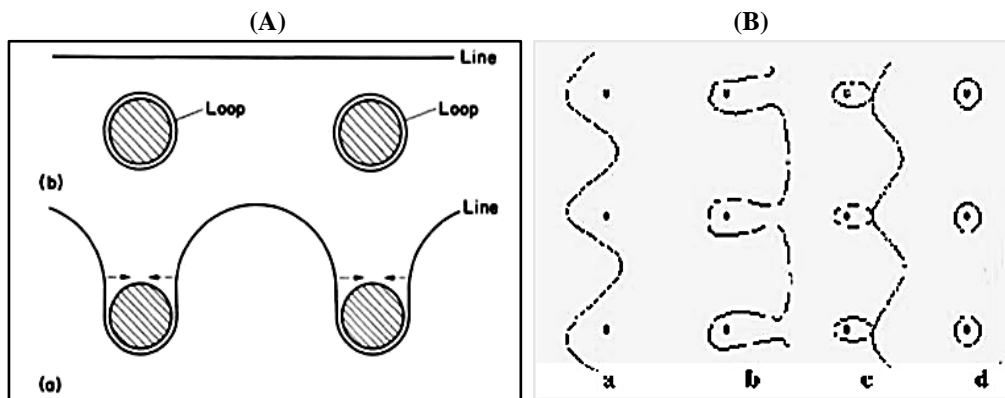
Figure4.Hardening mechanisms: (A) Orowan mechanism [38].; (B) Frank-Read mechanism

III. Precipitation Sequences in Aluminum Alloys.

Age-hardening aluminum alloys are characterized by very complex precipitation sequences that include several metastable phases. During sequences, several of these phases appear sequentially. On the other hand, the way in which these phases nucleate in the presence of the preceding phase is complicated. For example, in Al-Zn-Mg alloys, the presence of GP zones promotes the nucleation of η', while in Al-Mg-Si alloys, the presence of GP zones or groups of solutes inhibits the precipitation of β''. The most common technique for studying these precipitation sequences is differential scanning calorimetry, which measures the heat exchange between a sample and its surroundings during a thermal sequence. [39]. Generally, the aging of aluminum alloys includes four stages, namely: [40].

• Formation of groups of atoms;
• formation of Guinier-Preston (GP) zones;
• formation/growth of metastable phases;
• formation/coarsing of equilibrium phase.

For example, (Chen et al., 2009) **[41],** revealed the precipitation sequence in the aging of aluminum alloy 7055 shown in figures 5 and 6. It is obvious that in solid solution there are no precipitates. After aging for 5 min, nanometer-scale particles are observed within the grains, as shown in Figure 5(b). Selected Area Electron Diffraction (SAED) patterns indicate that the particles at this stage are primarily GP zones. After aging for 30 minutes, the GP zones increase in size and some of them transform into the η′ phase, as suggested by figures 5(c) and 6(a). After aging for 5 h, most of the precipitates observed in Fig. 5(d) are still the η′ phase, as suggested by the SAED pattern in Fig. 6(b). The η′ phase particles at this stage are much larger than those observed in the earlier stages and most of them have lost coherence with the Al matrix. After aging for 44 h, most of the η′ phase it transforms into coarse incoherent particles of the η-phase at equilibrium, as shown in Figs. 5(e), 6(c). For the exposed; 7055 aluminum alloy aged at 160°C exhibits the typical sequence:

$$\text{SSSS} \rightarrow \text{GP} \rightarrow \eta' \rightarrow \eta. \tag{3}$$

This sequence of phase transitions may vary slightly as the composition or aging process changes.
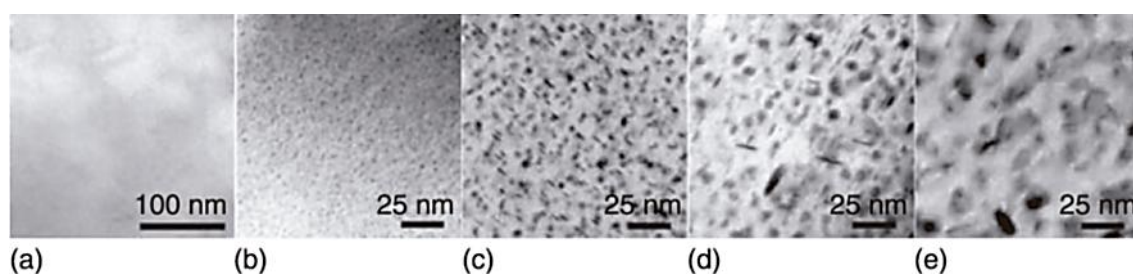
Figure. 5. TEM bright-fi eld images of precipitates in an AA7055 Al alloy aged at 160°C for different times: (a) solid solution treated; (b) aged for 5 min; (c) aged for 30 min; (d) aged for 5 h; (e) aged for 48 h**. [40]**
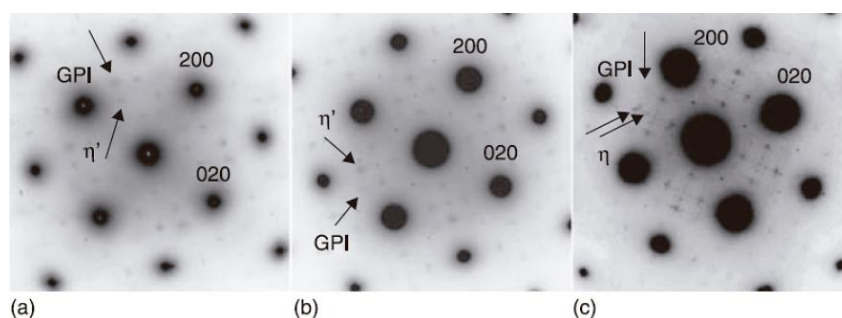
Figure.6, SAED patterns of AA7055 Al alloy aged at 160°C for different times: (a) 30 min <001> (b)5 h <001> (c) 48 h <001>. **[40]**

3.1. Precipitation in Aging Multicomponent Alloys.

The term "precipitation sequence" is based on the principle, for a given composition, the phase diagram predicts a stable phase that represents the end point of the reaction. The succession of these metastable phases, with the progressive loss of coherence, is usually called "precipitation sequence". In aluminum alloys, this sequence is sometimes unique to a given alloy system/family. **[42].**However, the word "sequence" is misleading because implies a fixed succession of reactions. More precisely it is to imagine a possible phase space in which the system chooses a "precipitation trajectory" depending on the conditions: composition, temperature history, mechanical processing and others. This is particularly true in complex multicomponent alloys, where the trajectories may choose to shorten some of the metastable phases or apparently jump from one precipitation sequence to another. Thus, for the Al-Cu-(Mg) system, it is proposed that the prototype precipitation sequence be: (4)

$$\text{SSSS} \rightarrow \text{GP zones} \rightarrow \theta'' \rightarrow \theta' \rightarrow \theta \ (\text{Al}_2\text{Cu}).$$
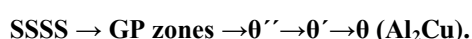
In this system, the GP zones are discs in the {100} planes, the precipitates θ˝ are coherent plates in the {100} planes where θ´ is semi-coherent and θ is incoherent with the aluminum solid solution. This alloy system is the basis for the 2xxx series family of alloys, which contain Cu and Mg [42]. In Fig.7, TEM image of the AA2196 alloy (high Li) is observed, after aging heat treatment (16 h at 155 °C). The diffraction patterns report that the microstructure of precipitates consists of a mixture of δ (Al3Li), θ (Al2Cu) and T1 (Al2CuLi), as can be seen in Fig. 2a and 2b.Another case of precipitation sequence is found in the Al-Zn-Mg-Cu alloy which, according to references [44–46], has been reported as follows:

$$\text{(SSSS)} \rightarrow \textbf{Guinier-Preston (GP) zones} \rightarrow \eta' \rightarrow \eta \tag{5}$$

GP zones usually form during natural aging and the early stage of artificial aging. Berg et al. [47] characterized the structure of two types of GP zones (GP-Ⅰ and GP-Ⅱ zones). GP-Ⅰ zones are fully consistent with the Al matrix and form over a wide temperature range: from room temperature to 141–151 °C. The GP-Ⅱ zones are considered layers rich in Zinc, according to the {111}Al planes and are formed by aging at temperatures above 71°C. It is generally believed that the GP-Ⅰ and GP-Ⅱ zones should be the precursors of the η' precipitates. However, early-stage precipitation remains controversial. Sha et al. [48] and Chen et al. [49] proposed that the transformation of small GP-Ⅰ zones into η' is the dominant mechanism.
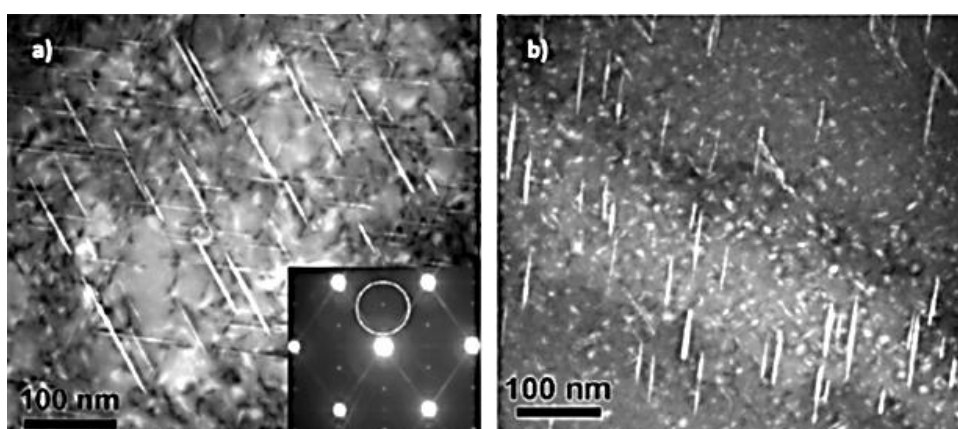
Figure7. (a) and (b) Darkfield TEM images of the AA2196 alloy after aging, viewed along a matrix zone axis of <110>;[43]

For the formation of precipitate η'. On the contrary, some investigations affirmed that the GP-Ⅱ zones are the main particles, as nucleation sites for metastable η' precipitates. [46, 47, 50].

IV. Aluminum alloys hardened by Aging

4.1. Serie 6xxx (Al-Mg-Si)

4.1.1. Series 6xxxSolubilized.

In the 6xxx series the homogenization (solubilized) has three main purposes: **1)** To reduce the microsegregation of the alloying elements, with the aim of dissolving the coarse primary Mg_2Si precipitates formed at the grain boundaries in the molten state; therefore, Mg and Si are evenly distributed, which is essential for subsequent artificial aging. [51,52]. **2)** Secondly, the intermetallic compounds: β-Al_5FeSi, which appear as needles in the microstructure, must be transformed into multiple precipitates: α-Al_{12}(Fe, Mn, Cr)$_3$Si, which appear in a more rounded shape with a variable stoichiometry [53].**3)** The third purpose is to allow the formation of nanoscale dispersoids [54] that have a decisive influence; thus, they can suppress the formation of coarse grains [55]. Dispersoids are particles whose size <1μm, and are incoherent precipitates that form during heat treatment up to solubilized temperature, whichare favorable only at nanometer scales.

The process of dissolution and phase formation that takes place depends on the composition of the alloy and is quite complex. Lodgarard et al. [54] found that during heating to the homogenization temperature, β′ precipitates nucleate homogeneously with subsequent growth, coarsening, and partial dissolution over a temperature range of approximately 100–350 °C. Upon reaching ~350 °C, intermediate u-phase precipitates form as the β′-precipitates dissolve. In this u phase, the dispersoids prefer to nucleate [54]. In parallel, the transformation of β-Al_5FeSi into α-Al_{12}(Fe, Mn, Cr)$_3$Si begins. Mn has been found to have the greatest influence on the β → α phase transformation during homogenization [53, 56, 57].

For the 6xxx series alloys, the homogenization temperatures are between 450 - 580 °C with different retention times [58]. As the alloy cools from the homogenization temperature, Mg-Si precipitates form in dispersoids,

where sub-grain boundaries and dislocations act as heterogeneous nucleation sites [59]. Therefore, the amount and size distribution of Mg-Si precipitates also depends on the number density of the dispersoids [60]. In Figure 8, the microstructure of the precipitates of an aluminum alloy AA6082 can be observed, identifying its composition, morphology and size. [61].
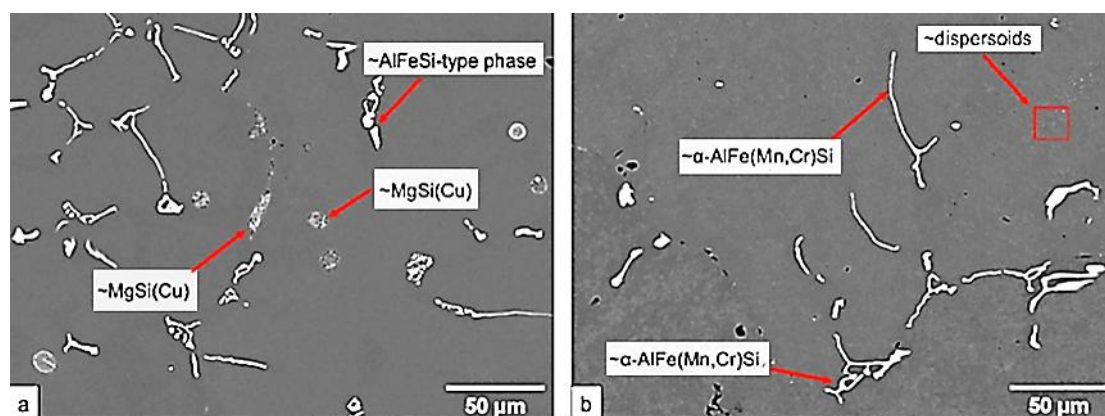
Figure8.BSE micrographs of AA 6082 aluminum samples; (a) as-cast microstructure showing the precipitates; (b) Microstructure homogenized at 540 °C for 4 h. Identification of the precipitated phases and the dispersoid zone. [61]

IV.1.2. Aged 6xxx series.

After giving enough time to the homogenate, a quenching is done at room temperature. Rapid cooling prevents the alloying elements from precipitating out, and also results in the formation of vacancies and solutes in the Al matrix. Then the solid solution becomes supersaturated (SSSS); that is, it is a supersaturated solid solution of magnesium, silicon and other elements in aluminum that forms at room temperature; but in a very unstable state. For precipitation hardening, vacancies are required to form the precipitates; therefore, the solid solution (SSSS) obtained after solubilization is a good option, since it gives rise to the formation of a large number of vacancies. The presence of vacancies increases diffusion and results in the formation of thickened solute clusters [62, 63] and dislocation loops [64-66].

During aging in these alloys; the Si forms initial groups, attracting slower Mg atoms, which causes co-groups to form, which then grow to become Guinier-Preston (GP) zones [62]. The GP zones are groupings of atoms in an orderly manner within the aluminum matrix that considerably strengthen the aluminum. GP zones (called clusters) are believed to be spherical in shape with an uncertain structure. The precipitation sequence in undeformed Al-Mg-Si alloys is as follows [67, 68]. The stoichiometric composition of this sequence of precipitates can be seen in table 2.

(SSSS) → atomicclusters → G-P zones (pre β″) →β″ → β′/ U1/ U2 /B → β, Si (estable). (6)
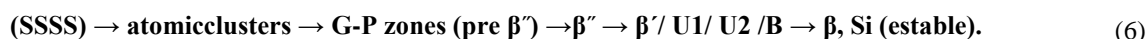
Table 2: Overview of precipitate phases in the Al-Mg-Si system Ref.[69]

Precipitation Sequences	Composition	Morphology	Crystal structure
SSSS	Unknown	Point Defect	FCC
Atomic Cluster	varying Mg and Si contents	Cluster	Unknown
GP zone	$Mg_xAl_{5-x}Si_6$	Spherical	Primarily monoclinic
β″	Mg_5Si_6	Needles	Body cantered monoclinic
β′	$Mg_{1.8}Si$	Rods	Hexagonal
U1	$MgAl_2Si_2$	Needle	trigonal
U2	MgAlSi	Rods	orthorhombic
B′	$Mg_{48}Al_6Si_{36}$	laths	hexagonal
β	Mg_2Si	Plates or cubes	FCC

Aging beyond maximum hardness is known as over-aging. In Al-Mg-Si alloys, it results in the transformation of β″ into a series of metastable phases such as β′, B′, U1, U2. The β′ precipitates that grow from the β″ category have a negligible contribution to the strengthening of the alloy; despite being thermally more stable and thicker than β″ with a length of ~500 nm [67]. The hexagonal β′ structure also grows along one of the <100> directions of the Al matrix [70, 71]. Subsequently, the β and Si phases are obtained in stable equilibrium,

after a sufficient aging time. The β phase is the intermetallic compound: Mg_2Si, that is presented in the form of platelets or in the form of cube and grows from the phases β´.
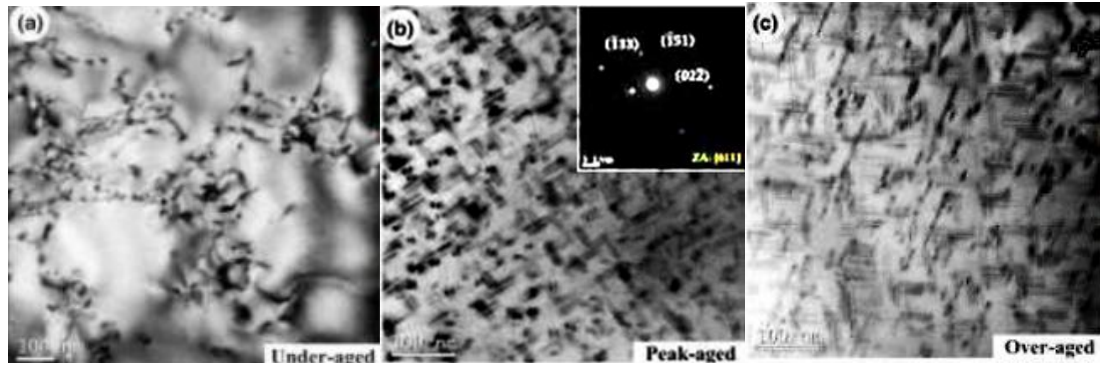
Figure9. Representative bright field TEM micrographs of 6063 alloy corresponds to 3 puntos de las zonas (a) underaged (100°C, 8 h), (b) peak-aged (175°C, 8 h) and (c) overaged (523 K, 8 h) Ref. **[72]**

These phases, due to their large size, do not contribute to the hardening or mechanical properties of the alloy. Figure 9 shows morphology corresponding to the three stages of aging.

In Al-Mg-Si alloys, the precipitation is complex and is influenced by the chemical composition and the thermomechanical treatment. The structures are modified by small additions of different elements added to the ternary structure generating another precipitation sequence. All the precipitates found under these conditions are structurally connected with the Si lattice, except for the main hardening phase that exhibits a partially discontinuous Si lattice. The added elements can be: (Li, Cu, Zn, Ge, Ag, Ni, Co and Au). If you add small percentages or traces of Cu to the Al-Mg-Si system, the maximum hardness increases, which correlates with the increase in the number density and volume fraction of the precipitates. The addition of Cu (0.4 wt%) alters the precipitation sequence of the Al-Mg-Si system as follows**[73, 74]**:

$$(SSSS) \rightarrow \text{atomic clusters} \rightarrow \text{G-P zones} \rightarrow β´´ + L + C + Q + QP + QC \rightarrow β´ + Q´ \rightarrow Q \qquad (7)$$
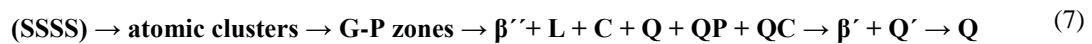
The stoichiometric composition of the precipitates of the previous sequence is shown in Table 3. This redistribution of solute suppresses the formation of β″ and forms different types of precipitates, L, C, QP and QC in maximum aging conditions, and Q ' in over aging condition. These precipitates are less consistent than β″ but can simultaneously be observed under certain chemical compositions and aging conditions. The L phase has a ribbon morphology and is a disordered structure **[74],** showing compositional variations. It has been shown that the L-phase has good thermal stability, and a correspondingly slower over aging. Furthermore, the L phase is formed in Mg-rich alloys containing Cu with high Mg/Si ratios (>2) **[75].** Phase C has a plate-like morphology with a monoclinic unit cell.**[76]** Both the L and C phases are elongated along <001>Al and have ahabitual plane <100>Al and are believed to be precursors to the Q' phase. It has been stated that the QP and QC phases are hexagonal and structurally connected to the Q' phase.**[77]** The QP phase is believed to be ~0.4 nm and the QC ~0.7 nm **[91].**

Table 3. Precipitate phases encountered in Cu containing Al–Mg–Si alloys. **[78]**

Phases	Compositions	Space Groups	Lattice parameters [nm]
GP zones	Variable	C2/m	$a = 1.48, b = 0.405, c = 0.648, β = 105.3°$
β″	$Mg_{6-x}Al_{1+x}Si_4$ $(0 \leq x \leq 2)$	C2/m	$a = 1.516, b = 0.405, c = 0.674, β = 105.3°$
β'	$Mg_{1.8}Si$	$P6_3/m$	$a = b = 0.715, c = 0.405, γ = 120°$
U1	$MgAl_2Si_2$	$P\bar{3}m1$	$a = b = 0.405, c = 0.674, γ = 120°$
U2	MgAlSi	Pnma	$a = 0.675, b = 0.405, c = 0.794$
B'	$Mg_9Al_3Si_7$	Hexagonal	$a = b = 1.04, c = 0.405, γ = 120°$
β	Mg_2Si	$Fm\bar{3}m$	$a = 0.635$

IV.2. Serie 7xxx (Al-Zn-Mg (Cu))

The 7xxx series alloys contain two families, the Cu-free Al-Zn-Mg alloys and the Cu-containing Al-Zn-Mg-Cu alloys. This last family is the one that provides the strongest hardening of all families of aluminum alloys. $η´$ precipitates rich in Mg and Zn provide maximum hardening, and higher strength can be achieved by maximizing

the volume fraction of these precipitates [79]. It has been shown that in the cooled state there is an excess of Mg, Zn and Cu at the grain boundaries by a factor of about 2-3 [80]. The precipitates that form are not stoichiometric compounds, but contain Al, Mg, Zn and Cu.[80]. The precipitates also have a regular layered structure [81]. Only with excessive over aging the precipitates become enriched in Cu [82].

IV.2.1. Serie 7xxx: Solubilized and quenching.

Regarding the solubilization and homogenization of the aluminum alloys 7XXX series, information is still lacking. Most research has focused on qualitative studies of microstructural evolution and phase transformations during homogenization[83]. A.R. Eivani et al., [83], carried out a study on the evolution of the phases in the homogenization treatment of the AA7020 alloy. The treatments were isothermal and were carried out at 390 °C, 430 °C, 470 °C, 510 °C and °550 C for 2, 4, 8, 16, 24 and 48 hours. At 470 °C, the volume fraction was almost constant, while at 510 °C and 550 °C decreased. Figure 10 shows images of the dominant phases that formed during homogenization at low temperature of 390 °C.The morphology of these precipitates is round and needle-shaped. The formation of these precipitates is attributed to the supersaturation of the structure with alloying elements, due to microsegregation during solidification with high cooling rates applied during casting. It was also found that, after homogenization at a high temperature, 550 °C, some of the particles did not dissolve in the structure, because they were retained at the GB grain boundaries. It is concluded that at low homogenization temperatures there is an increase in the fraction of precipitated particles of $MgZn_2$ (η) and Mg_2Si (β). However, at high temperatures, the precipitates η and β not form.
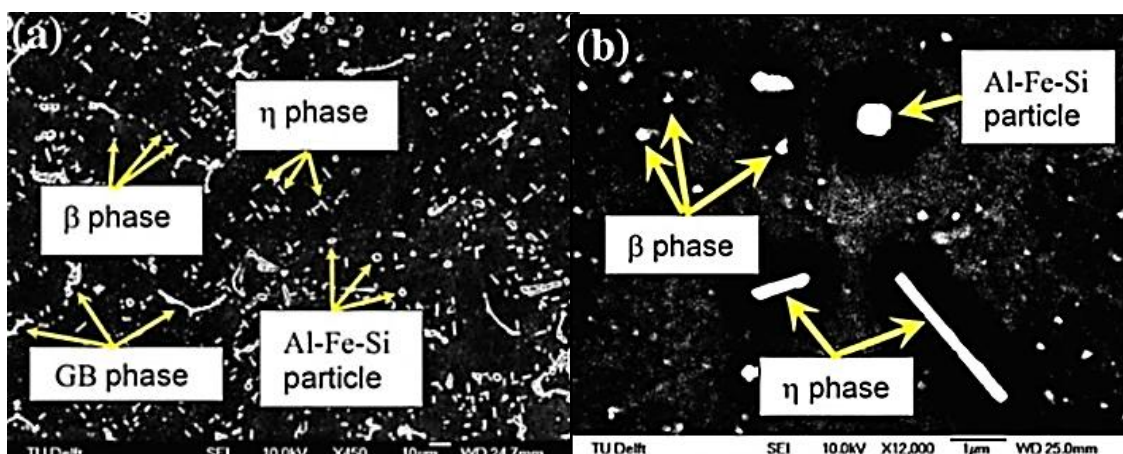
Figure 10.(a) Image FEG-SEM of homogenized AA720 aluminum at 390 °C, and (b) round, needle-shaped $MgZn_2$ (η) and Mg_2Si (β) particles together with large Al-Fe-Si particles [83]-

Regarding the quenching of 7XXX alloys, it has been reported when the quenching time is long or the quenching speed is slow, η phase easily precipitated at the grain boundaries of these alloys; effect that is harmful to the hardening of the alloy and promotes a high sensitivity to intergranular corrosion [84]. Therefore, the quenching time must be strictly controlled and the temperature does not must fall in the range of quenching sensitivity of the alloy [84-86]. Figure 11 shows the precipitation of the η phase at the grain boundaries, showing that the more time is spent in the cooling rate, the more η phase content precipitates at the grain boundaries.
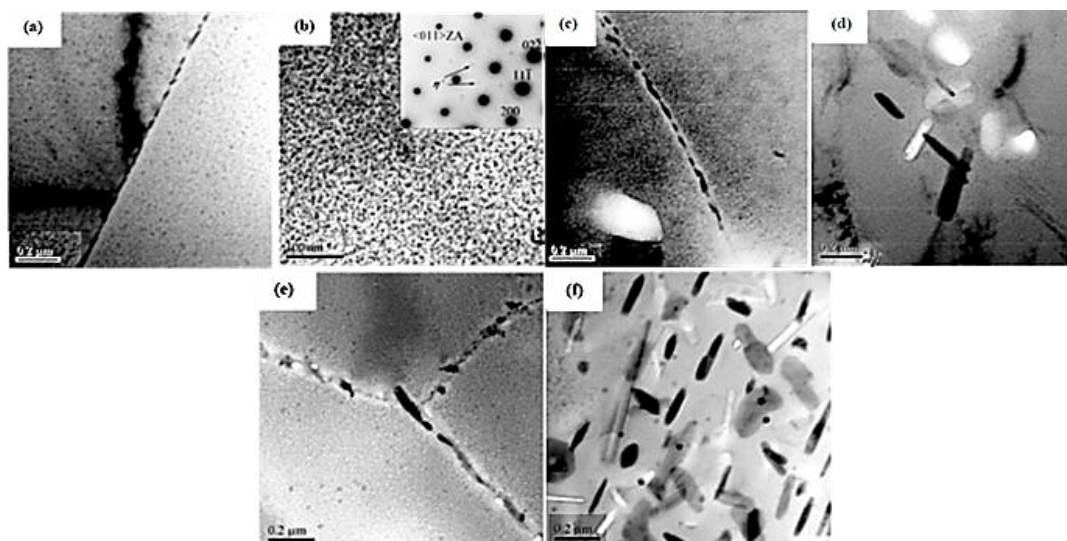
Figure 11. TEM images showing grain and sub-grain boundary precipitates in 7050-T6 alloys treated with different transfer times (a,b) 2 s, (c,d) 45 s, (e,f) 120 s. **[87].**

4.2.2. Aged 7xxx serie.

The hardening and mechanical resistance of 7xxx series aluminum alloys is determined, mainly by the precipitation of the matrix and the evolution of the microstructure according to the precipitates during the natural or artificial aging treatment, after the solution treatment at 460- 490 °C and cooling with water. **[88].** The general sequence of precipitation in the 7xxx series aluminum alloy **[89]** is:

$$\text{(SSS)} \rightarrow \text{zonas G.P.} \rightarrow \text{metastable phase} \eta' \rightarrow \text{equilibrium phase (phase } \eta) \tag{8}$$
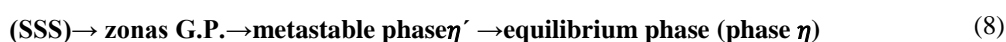
The main strengthening phase is the η'' phase. Furthermore, it is widely accepted that this treatment is capable of modifying the size, volumetric fraction and distribution of the precipitates**[90- 96].**

If the particular case of the precipitation sequence of the 7A85 alloy is examined, it can be generalized that for the Al–Zn–Mg–Cu alloy the precipitation sequence is that shown previously [97–99]. Berg et al. **[100]** characterized the structure into two types of GP zones (GP- Ⅰ and GP- Ⅱ zones). GP- Ⅰ zones are fully consistent with the Al matrix and form over a wide temperature range, from room temperature to (141–151) °C. The GP- Ⅱ zones are considered zinc-rich layers in the {111}Al planes and are formed by aging at temperatures above 71°C. It is generally believed that the GP- Ⅰ and GP- Ⅱ zones should be the precursors of the η′ precipitates. However, early-stage precipitation remains controversial. Sha et al. **[101]** and Chen et al. **[102]** proposed that the transformation of small GP- Ⅰ zones into η′ is the dominant mechanism for the formation of η′ precipitate. On the contrary, some investigations stated that GP- Ⅱ zones are the main particles as nucleation sites for metastable η' precipitates **[99, 100, 103].**

Images of the 7A85 **[104]** alloy sample aged at 161°C for 1 h are presented in Figure 12. As seen in Figure 12(a), the distribution of precipitates is presented in the (BF) image. From the insert graphs it can be known that the width of most of the precipitates is between 3nm - 6nm and the average size is 4.79nm. These precipitates were observed in detail in Figure 12(b) in different areas (C, D, E) and the corresponding diffraction patterns were obtained (Fig. 2(c-e)). Showing that the area represents the Al matrix. That there is a round shaped precipitate in zone D. The corresponding diffraction pattern shows a continuous line along the <111>Al direction. The image and diffraction pattern corresponding to zone D is sufficient to confirm that the precipitates are GP- Ⅱ zones**[105, 106, 107].**

The stable precipitate η has a hexagonal lattice with a= 0.521 nm and c = 0.860 nm and a chemical composition of MgZn2. The metastable η' and GP zones are believed to be responsible for the maximum hardening effect of these alloys. Crystal structure models for the metastable η' phase have been proposed **[108 - 110].**
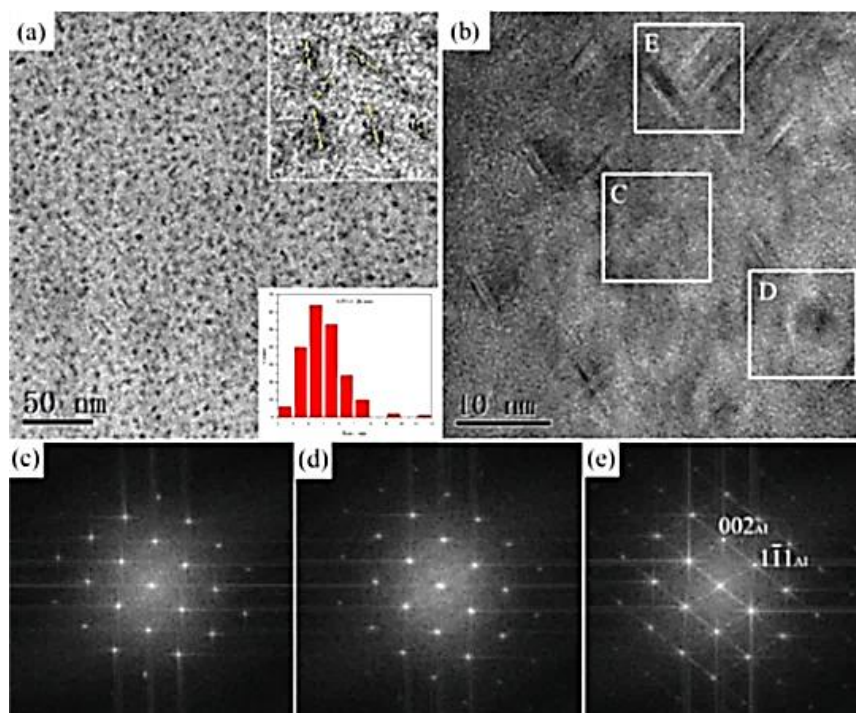
Figure12. Aluminum sample 7A85 aged at 164°C for 1 h. (a) BF image taken in the [110]Al direction; (b) HRTEM image obtained along the axis of the [110]Al zone in the Al matrix of the sample; (c-e) diffraction patterns obtained from three different areas shown in (b). **[104]**

A hexagonal cell structure for η' with: a= 0.496 nm and c = 1.402 nm has been commonly accepted, but there is still controversy about its stoichiometry.**[11,112].** Two types of GP zones have been reported in ternary Al alloys, but our understanding of their structures and chemistry remains limited.**[113].** Gang Sha et al., **[114]** conducted a study on the characterization of precipitates in artificial aging applied to alloy 7050. They found that early-stage precipitates present after a stabilization aging treatment at 121 °C for 4 h have a crystallographic structure similar to η', but probably rich in defects. After the T6 treatment, with double aging at 121 °C for 24 h followed by 12 h at 154 °C, the η and η' phases coexist within the Al matrix. Figure 1 shows that for this material that contains traces of Si, Zr and Fe; after doing a statistical analysis; it was observed that the precipitates in Figure 1(b) have a wide size range: from 3 to 15 nm. They are small, thin, elongated precipitates ~3 nm long and 1–2 nm thick, randomly distributed. The analysis of the diffraction pattern indicated the coexistence of the two types of precipitates η and η'.

IV.3. Serie 2xxx (Al-Cu-Mg)

4.3.1. Serie 2xxx: Solubilized and Quenching.

Heat treatment of aluminum alloys includes (in sequence): solution treatment, quenching, and ageing. However, non-homogeneous conditions in the first two processes affect precipitation behaviors during aging **[115, 116]**. A low cooling rate during quenching leads to precipitation, and a decrease in the solid solubility of Cu in 2xxx alloys **[117].** The study **[118]** done on the Al-Cu-Li alloy reveals that a non-homogeneous distribution of the chemical composition results in the formation of different phases and a non-uniform influence on corrosion. Furthermore, studies **[119-121]** indicate that a low cooling rate leads to the formation and coarsening of cooled precipitates and decreases the corrosion properties of Al-Cu-Mg alloy and the yield strength of Al-Cu-Mg alloy. Cu-Cd. Therefore, the precipitation behaviors of Al-Cu alloys are affected; both by the segregation that occurs during solubilization and
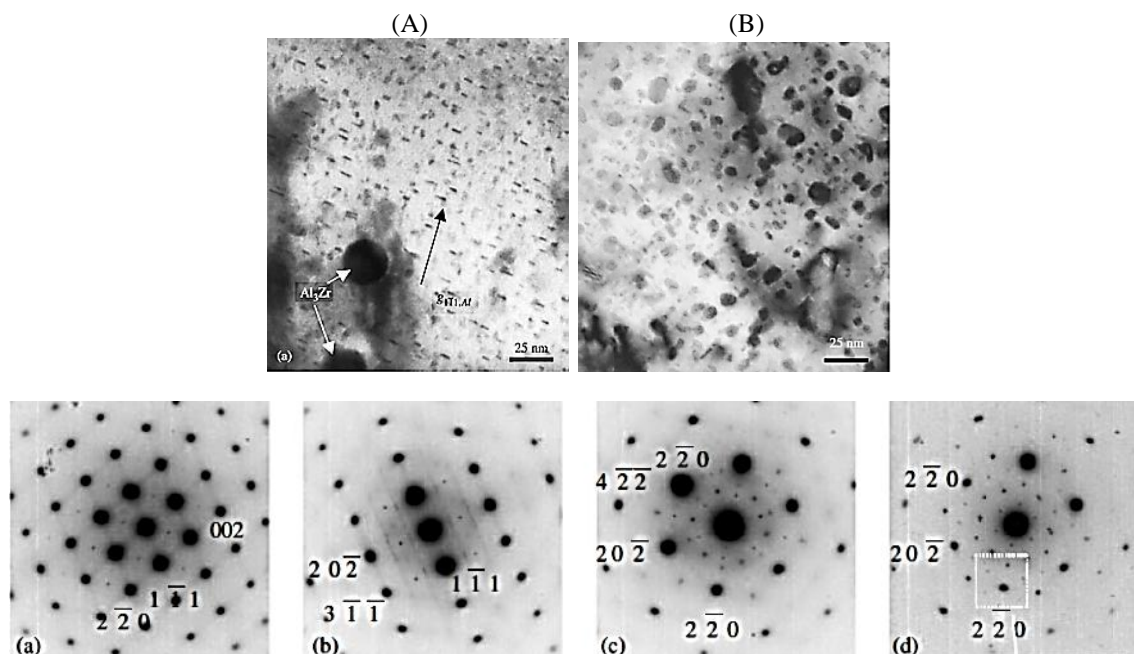
Figure 13. Images TEM :(A)After the stabilization treatment, Al3Zr precipitates in the Al matrix. (B) TEM image of a sample aged up to T6 observed in the axis of the <111> zone c); Selected-area diffraction patterns of the alloy under stabilization treatment: (a) [110]; (b) [121]; (c) [111]; (d) [111] SAD from η particles on grain boundary. Diffraction pattern of selected areas. **[114]**

by the rate of cooling during quenching. Al-Cu alloys are usually solution treated in the solvus and eutectic temperature range **[122].** Figure 13 shows the microstructure of the AA7050 alloy after solution stabilization.

4.3.2. Artificial Aging.

For this series of aluminum alloys, the precipitation sequence is very diverse and includes many factors. The predominant factor is the Cu/Mg ratio. Several experimented cases are presented: In the Al-Cu-Mg alloy AA2519 with a Cu/Mg rate (≥ 5.6) it presents the following sequence of precipitation from the solubilized solid solution (SSSS): **[123,124]** in the following way:

$$\text{SSSS} \rightarrow \text{GP zones (Al}_3\text{Cu)} \rightarrow \theta''(\text{Al}_3\text{Cu}) \rightarrow \theta' (\text{Al}_2\text{Cu}) \rightarrow \theta (\text{Al}_2\text{Cu}) \tag{9}$$
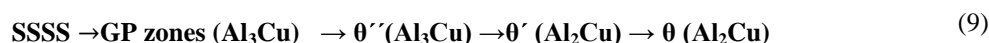
With this precipitation, the increase in mechanical resistance and ductility is achieved; effect that could be partially attributed to the decrease in the volume fractions of the primary phase (θ) formed during solidification, since the Cu content in the AA2519 alloy is close to the solubility limit of this element in the matrix and also to the positive effect of Mg on the precipitation structure. However, despite numerous research works **[126-132],** the precipitation behavior of the AA2519 alloy remains poorly understood.Figure 14(b) shows the inclusion of the Ω phase, with a longer aging time. Only under certain circumstances, this Ω(Al$_2$Cu) phase can appear in the second precipitation sequence **[124, 126, 133].** This phase is totally coherent with the Al matrix, forming thin hexagonal plates in the {111}α planes **[124, 134]**. The Ω phase is assumed to be the most effective reinforcing phase in Al-Cu-Mg-Ag alloys **[135].** The Ω phase has an orthorhombic lattice (a = 0.496 nm, b = 0.859 nm, c = 0.848 nm) **[124, 133]** with very small differences in atomic coordinates from the equilibrium θ phase. The Ω phase is a variant of the equilibrium phase θ (Al$_2$Cu) and its nucleation mechanism occurs on a group of atoms (called clusters) rich in magnesium. The role ofmagnesium on the structural evolution of this phase has not been clearly understood, but it is believed to be an essential component for the formation of the Ω phase **[136].**
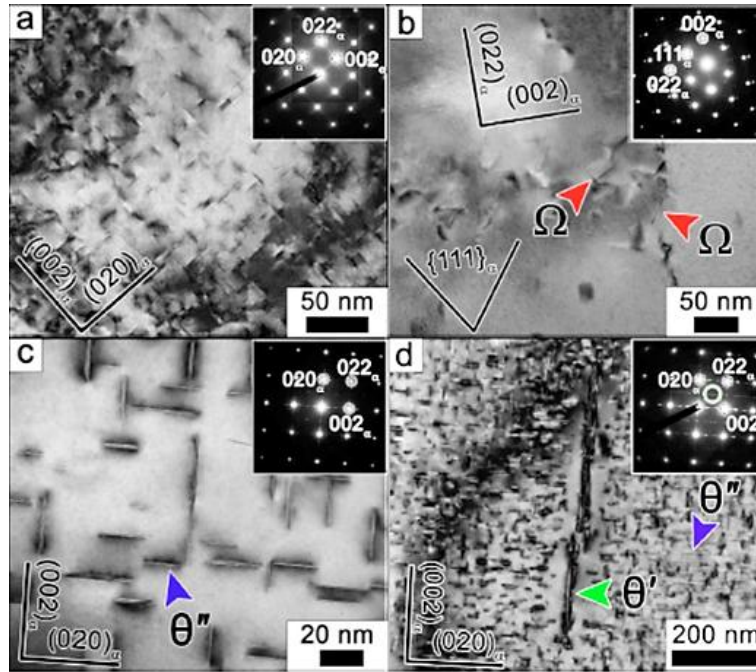
Figure14.BF-TEM micrographs of aluminum alloy AA2519. SAED patterns recorded on artificially aged samples are shown: (a, b) 0.5 h at 190 °C; (c, d) 3h, 190°C. Blue, green and red arrows indicate phase plates θ´´ - θ´ - Ω respectively **[125]**

In Al-Cu-Mg AA2618 alloy with a Cu/Mg ratio = 2.2, presents the following conventional generalized precipitation sequence, starting from solubilized solution (SSSS): **[137 ,138]**

$$SSSS \rightarrow Zones \rightarrow S´´ \rightarrow S´ \rightarrow S \qquad (10)$$

The zones, which are matrix-coherent and enriched with copper and magnesium, were named Guinier-Preston-Bagaryatsky (GPB) zones by Silcock.**[139]** The ternary S phase (Al2CuMg) is the equilibrium intermetallic phase, which has an orthorhombic structure with lattice parameters: a = 0.400 nm, b = 0.923 nm, c = 0.714 nm.**[140].** The two intermediate phases, S´´ and S´, are considered to have a slightly distorted S structure with different degrees of coherence with the Al matrix. **[137, 138]**The S´ phase precipitates with orientation relationships [100]S´//[100]α [010]S´//[021]α, and [001]S´//[012]α. **[137].** Silcock, however, found no evidence of an S"-like phase in Al-Cu-Mg alloys**.[139];** Instead, an intermediate phase between the GPB zones and the S´ phase was identified in the precipitation sequence. This phase, called GPB2 zones, can be developed in situ from the GPB zones. Subsequently, Charai et al.**[141]** identified the S´´ phase in an Al-0.9% Cu-1.4% Mg (w%) alloy by high resolution microscopy (HREM), while the GPB2 zones were identified in different Al-Cu-Mg alloys.**[142, 143].** Shih et al.**[144]** and Wang et al.**[145]** designated GPB2/S´´ as the intermediate phase between GPB and S´. According to the experimental studies of H. Lu et al, **[146]**, the structural changes during the artificial aging of the Al-Cu-Mg alloy (AA2618) with Cu/Mg rate = 2.2 were better defined according to the following sequence:

$$SSSS \rightarrow clústers + GPB \rightarrow GPB + GPB2 \rightarrow GPB2 + S´ \rightarrow S´ + S \rightarrow S. \qquad (11)$$
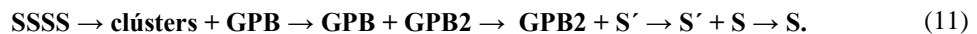
Where: [(GPB)= Guinier–Preston–Bagaryatsky zones]

Figure 15(a) shows a -BFI TEM of an aging peak of alloy AA2618 (20 h, 200 °C). The diffraction pattern confirms the existence of precipitate S'. Figure 15(b) shows the same overaged alloy (80h, 200°C) where the precipitate S' disappears and gives rise to the stable phase S.
With the background shown, it is observed that the sequence of precipitates not only depends on the chemical composition of the alloy but also on other aging parameters.
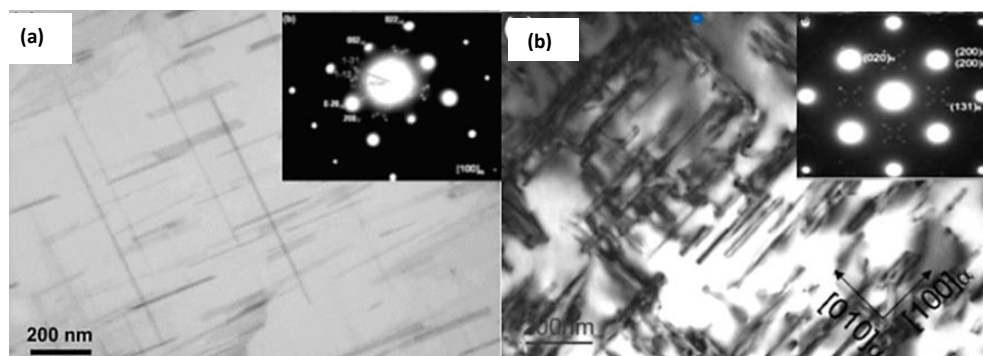
Figure 15. TEM micrographs of the AA2618 alloy: (a) aged (20 h -200C). Its diffraction (SADP) taken near the [100]α axis is observed. Sheet-like precipitates were identified as the S' phase. (b) Image taken for an overaged sample, (80 h - 200 °C), the SADP located near the [001]α axis. The existence of the S phase was identifiedmoreover of the Al matrix **[146]**

4.4.4. GP and GPB Zones

GP zones are coherent groups rich in solutes. They have the same crystal structure and lattice orientation as the matrix phase. Generally, the GP zones are not the equilibrium phase. GP zones are best known for their appearance in cubic fcc lattices, they also appear in (bcc) arrays; For example, Fe-based aluminum alloys **[147]**
The formation of GP and GPB zones in Al-Cu-Mg alloys proceeds rapidly at room temperature immediately after quenching. This evolution of the structure is well known for GP zones but not for GPB zones. The formation of both zones, arefound in the α-θ (GP) and α-S (GPB) phase fields, respectively. However, these zones that form so easily at room temperature are unstable upon aging at higher temperatures,in either θ phase or S phase **[148].**
The sequence and structures of the precipitates that evolve in α-θ alloys, α→GP→θ″→θ′→θ, (where θ ≡Al2Cu), are now undisputed **[149].** However, the same does not happen with α-S alloys that have an α→GPB→S evolution sequence, where the analogue of the (GP) zones are the Guinier-Preston-Bagaryatsky (GPB) zones and S ≡Al$_2$CuMg. These GPB zones have a recently described structure with some precision.**[150, 151]**. Its morphology is rod or needle-shaped, but observed only after alloy treatment at temperatures > 180°C. However, in some cases of natural aging, very soon after saturated solution quenching (STQ), GPB zones have also been observed [152]. Figure 16(a) illustrates a photomicrograph of the GP zone and Figure 16(b) shows the distortion of the lattice. Figure 17 shows an imagen TEM whereis observed GPB zone in aged alloy sample.
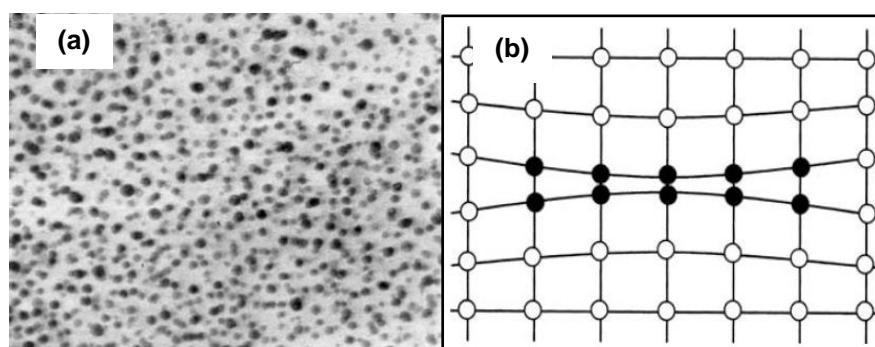
Figure 16.(a)TEM micrograph of an Al-4.4% Ag alloy thin film, quenched with water at 525 °C and aged for 5 days at 160 °C, showing 85 Å diameter spherical GP zones; (b) Elastic distortion associated with the GP zone**[153]**
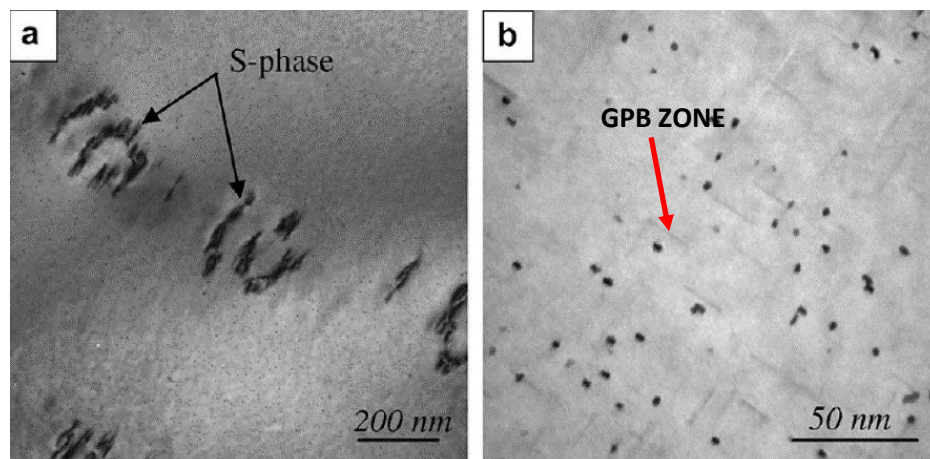
Figure 17. Typical features of the microstructure after 96 h aging at 180 C. (a) Agglomerates of S-phase particles that nucleated in dislocation loops; (b) small needle-shaped particles (GPB zones) **[157]**

According to Bagaryatsky**, [154, 155],** in Al-Cu-Mg alloys, the first phase to form (now called Guinier-Preston-Bagaryatsky (GPB) zones) has an atomic arrangement, in which Cu and Mg populate the plane of the matrix {100}Al, in a similar way to stable S phase that form in plane {100}S. Silcock **[156]** has provided a different interpretation for GPB zones. GPB zones were predicted to be rod-shaped particles, 1 - 2 nm in diameter and 4 - 8 nm in length. It was proposed that GPB zones can be interpreted as having a tetragonal lattice with parameters a = 0.55 nm, c = 0.404 nm [156]. GPB zones **[155]** were found to form only with high-temperature aging **[156].** The structure of GPB [155] was proposed to be related to the cubic phase Mg2Al5Cu5. Figure 1(a) shows the S phase that results from aging at 180°C for 96 h. In Fig. 1(B) needle-shaped particles (GPB zones) are observed.

IV. Conclusion

Precipitation hardening is produced by the effect of precipitated particles, as long as they are coherent and coplanar with the matrix. These precipitates deform the crystalline planes of the matrix in their surroundings and produce hardening.

The ″precipitation sequence″. in aluminum alloys, are sometimes reported as fixed for a given alloy system. More precisely it is to imagine that the system chooses a "precipitation trajectory" depending on the conditions: composition, temperature history, mechanical processing history and so on, as is the case of the Al-Mg-Si and Al-Cu-Mg sequences shown below.

(SSSS) → clusters → GP zones (pre β″) →β″ → β′/ U1/ U2 /B → β, Si (stable).

(SSSS) → clústers + GPB → GPB + GPB2 → GPB2 + S′ → S′ + S → S

Despite numerous research papers; the precipitation behavior of certain alloys remains poorly understood. The same happens with many precipitated phases that are not yet defined, such as the Ω phase, which is said to be a variant of the equilibrium phase θ (Al$_2$Cu) and its nucleation occurs on a group of atoms (called clusters) rich in magnesium. The role of magnesium on the structural evolution of this Ω phase has not been clearly understood to date.

Respect for the GP and GPB zones. First, they form in almost all precipitation sequences of age-hardenable aluminum alloys. But; although, the GP zone is well defined for all sequences of precipitates in heat treatable alloys; the GPB zone appears only in certain sequences, and in some of them it gives rise the formation of a second GPB2 zone. There is still controversy among researchers regarding the stoichiometry and requirements for the formation of the GPB and GPB2 zonesin the precipitate evolution sequence during the aging of aluminum alloys.

References

[1]. Sato T (2010), ' Innovative development of aluminum research and technologies in Japan ' in Kumai S , Umezawa O , Takayama Y Tsuchida T. and Sato T , (eds), 12th International

[2]. Conference on Aluminum Alloys , 5–9 September 2010 , Yokohama, Japan. Tokyo : Japan Liu Q and Lin L (2010), ' Current status of research and industries of Al sheets in China ', 12th InternationalConference on Aluminum Alloys , 5–9 September 2010 , Yokohama, Japan. Tokyo : JapanInstitute of Light Metals , 20 – 29 .

[3]. Hirsch J and Laukli H I (2010), ' Aluminum in innovative light-weight car design ', in Kumai S , Umezawa O , Takayama Y , Tsuchida T. and Sato T , (eds), 12th InternationalConference on Aluminum Alloys , 5–9 September 2010 , Yokohama, Japan. Tokyo : Japan Institute of Light Metals , 46 – 53 .

[4]. Smith, W.F., "Fundamentos de la Ciencia e Ingeniería de Materiales", McGraw-Hill Interamericana, 3ª edic. España 1998.

[5]. Askeland, D.R., "La Ciencia e Ingeniería de los materiales", Grupo Edit. Iberoamérica.

[6]. Reed-Hill, R.E., "Principios de Metalurgia Física", Comp. Edit. Continental, 2ª impresión, México, D.F. 1971.

[7]. Porter, D.A. y Kenneth, E.E., "PhaseTransformation in Metals and alloys", Van Nostrand Reinhold, UK, 1984.

[8]. Shewmon, P.G., "Transformation in Metals", McGraw-Hill Book Company. USA, 1969.

[9]. American Society for Metals, "Metals Handbook", Vol. 2, 8th Edition, p-.p. 271-283

[10]. Quiong Li and F.E. Warner, Journal of Materials Science, Vol 32, pp 301-309, 1991.

[11]. Callister William, "Introducción a la ciencia e ingeniería de los materiales", Ed. Reverté, Tercera edición, pp. 74, 349-355, 375-378, Barcelona España, 2001.

[12]. Ojeda Ramírez, B., endurecimiento por precipitación de aleaciones de aluminio, tesis que para optar por el grado de: Maestra en Metalurgia, Universidad Nacional Autónoma de México, 2014.

[13]. Lumley. R.N. and Polmear, I.J.(2004), The Effect of LongTerm Creep Exposure on the Microstructure and Properties of an Underaged Al-Cu-Mg-Ag Alloy, Scripta Mater., 50, 1227-1231.

[14]. Lumley, R.N., O'Donnell, R.B., Polmear, I.J. and Griffiths J.R (2005), Enhanced Fatigue Resistance by Underageing an Al-Cu-Mg-Ag Alloy, Mater. Forum, 29, 256-261.

[15]. Aleaciones de Aluminio, Disponible en la página Página Web: http://www2.ing.puc.cl/icmcursos/metalurgia/apuntes/cap5/50/

[16]. Loeffler, H., Kovacs, I. and Lendvai, J. (1983), Decomposition Processes in Al-Zn-Mg Alloys, J. Mater. Sci., 18, 2215-2240.

[17]. Lynch, S.P. (1991), Fracture of 8090 aluminum-lithium plate I. Short transverse fracture toughness, Mater. Sci. Eng A, A136, 25-43.

[18]. J. Polmear, "From atoms to aeroplanes", (Cominicated to The Royal Society of Victoria on Thursday, 9 September 1999)

[19]. Wang, S.C. and Starink, M., "Two types of S phase precipitates in Al–Cu–Mg alloys", Acta Mater., 55, 2007, p.933.

[20]. Silckok, J.M., J. Inst. Met., 88, 1961, p.357

[21]. FENG, Z.Q., YANG, Y.Q., HUANG, B., HAN, M., LUO, X., RU, J.,"Precipitation process along dislocations in Al–Cu–Mg alloy during artificial aging", Mater. Sci. Eng: A, 528, 2010, p.706.

[22]. Hong-ying, L., Jie, B., Yang-kuo, Z. y Xiao-feng, W., "Establishment of continuous cooling transformation diagrams of aluminum alloys using in situ Voltage measurement", Transactions of Nonferrous Metals Society of China, August 2011,p.p. 1944-1949.

[23]. Yu-hua, Z., Shu-cai, Y., y Hong-zhi, J. "Microestructure evolution in cooling process of Al-Zn-Mg-Cu alloy and kinetics description", Transactions of Nonferrous Metals Society of China, April 2012, p.p. 2087-2091

[24]. Dolan, G.P. y Robinson, J.S., "Residual stress reduction in 7175-T73, 6061-T6 and 2017A-T4 aluminum alloys using quench factor analysis", Journal of Materials Processing Technology, 2004, p.p. 346-351.

[25]. G. KOSTORZ, "Phase Transformations in Materials" Wiley-VCH, Federal Republic of Germany, (2001) pp 371.

[26]. P.W. VOORHEES, Annu. Rev. Mater. Sci. 22 (1992) pp. 197-215.

[27]. A. UMANTESEV, "Thermal Effect of Phase Transformations: A review", Physical D 235, (2007) pp. 1-14.

[28]. A. K. JENA, M.C. CHATURVEDI, "Transformaciones en los materiales", Prentice Hall. SA (1992) pp. 301-302

[29]. W.F. Smith., Principles of material science and engineering, Mc Grow – Hill, 1996, 528.

[30]. VARGEL, C., Corrosion de l'aluminium, Paris, 2004.

[31]. A. K. Jena, M.C. Chaturvedi, "Transformaciones en los materiales", Prentice Hall. USA (1992) pp. 301-302

[32]. W. Callister, "Introducción a la ciencia e ingeniería de los materiales", Ed. Reverté, Tercera edición, pp. 74, 349-355, 375-378, Barcelona España, 2001.

[33]. E. A. Starke Jr, Treatise on Material Science Technology vol. 3 (1988) 35.

[34]. Gao X. Nie J.F., Muddle B.C., "The Effect of Si additions on Ω precipitation in Al-Cu- Mg-(Ag) Alloys" Mater Sci Forum 217-222, 1996

[35]. Chee Fai Tan, and Mohamad R. Said., Effect of Hardness Test on Precipitation Hardening Aluminum Alloy 6061-T6, Chiang Mai J. Sci. 2009; 36(3) : 276-286

[36]. [ASM Handbook, Volume 4: Heat Treating- p 841-879, 1991]

[37]. Qiong Li, and F. E. Wawner, "Characterization of a cubic phase in an Al-Cu-Mg-Ag alloy" journal of Mareials Science, Vol 32, pp. 5363- 5370, 1997.

[38]. D. Hull and D.J. Bacon, Introduction to Dislocations 3rd ed., Butterworth Heinemann, 1999

[39]. [Geoge Totten] Handbook of Aluminum, Volume 2, 2003, ISBN: 0-8247-0896-2, p.177.

[40]. Xianna Meng et all., Influence of solution treatment on microstructures and mechanical properties of a naturally-aged Al–27Zn–1.5Mg1.2Cu–0.08Zr aluminum alloy, Materials Science & Engineering A 802 (2021) 140623

[41]. Chen J Z , Zhen L , Yang S J , Shao , W Z and Dai S L (2009), ' Investigation of precipitationbehavior and related hardening in AA 7055 aluminum alloy ', Materials Science and Engineering A , 500 , 34 – 42 .

[42]. Christophe Sigli, et all., Recent advances in the metallurgy of aluminum alloys. Part II: Age hardening, C.R.Physique19(2018)688–709

[43]. B. Decreus, A. Deschamps, F. De Geuser, P. Donnadieu, C. Sigli, M. Weyland, The influence of Cu/Li ratio on precipitation in Al–Cu–Li–x alloys, Acta Mater. 61 (2013) 2207–2218.

[44]. A.Khalfallah,A.A.Raho,S.Amzert,A.Djemli,PrecipitationkineticsofGPzones,metastableη′phaseandequilibriumηphaseinAl-5.46wt%Zn–1.67wt%Mgalloy,Trans.NonferrousMet.China29(2)(2019)233–241.

[45]. Y.S.Lee,D.H.Koh,H.W.Kim,Y.S.Ahn,Improvedbake-hardeningresponseofAl–Zn–Mg–Cualloythroughpre-agingtreatment,Scr.Mater.147(2018)45–49.

[46]. J.Z.Liu,J.H.Chen,X.B.Yang,S.Ren,C.L.Wu,H.Y.Xu,J.Zou,RevisitingtheprecipitationsequenceinAl–Zn–Mg–basedalloysbyhigh-resolutiontransmissionelectronmicroscopy,Scr.Mater.63(11)(2010)1061–1064.

[47]. L.K. Berg, J. Gjonnes, V. Hansen, X.Z. Li, M. Knutson-Wedel, G. Waterloo, D. Schryvers, L.R. Wallenberg, GP- zones in Al–Zn–Mg alloys and their role in artificial aging, Acta Mater. 49 (17) (2001) 3443–3451.

[48]. G. Sha, A. Cerezo, Early-stage precipitation in Al–Zn–Mg–Cu alloy (7050), Acta Mater. 52 (15) (2004) 4503–4516.

[49]. J. Chen, L. Zhen, S. Yang, W. Shao, S. Dai, Investigation of precipitation behavior and related hardening in AA 7055 aluminum alloy, Mater. Sci. Eng. A 500 (1–2) (2009) 34–42.

[50]. M. Liu, B. Klobes, K. Maier, On the age-hardening of an Al–Zn–Mg–Cu alloy: a vacancy perspective, Scr. Mater. 64 (1) (2011) 21–24.

[51]. J. Røyset, U. Tundal, C. Espezel, O. Reiso, Al-Mg-Si billets with high extrudability– state of the art and beyond, Mater. Today Proc. 10 (2019) 185–192.

[52]. I. Polmear, D. StJohn, J.-F. Nie, M. Qian, Light Alloys: Metallurgy of the Light Metals, Butterworth-Heinemann, 2017.

[53]. N.C.W. Kuijpers, F.J. Vermolen, C. Vuik, P.T.G. Koenis, K.E. Nilsen, S. Van Der Si transformation kinetics in alloying elements, Mater. Sci. Eng. A 394 (2005) 9–19.

[54]. L. Lodgaard, N. Ryum, Precipitation of dispersoids containing Mn and/or Cr in Al– Mg–Si alloys, Mater. Sci. Eng. A 283 (2000) 144–152.

[55]. M. Kenyon, J. Robson, J. Fellowes, Z. Liang, Effect of dispersoids on the microstructure evolution in Al–Mg–Si alloys, Adv. Eng. Mater. 21 (2019) 1800494.

[56]. N.C.W. Kuijpers, F.J. Vermolen, K. Vuik, S. Zwaag, A model of the β-AlFeSi to α-Al (FeMn) Si transformation in Al-Mg-Si alloys, Mater. Trans. 44 (2003) 1448–1456.

[57]. Niels Cees Willen Kuijpers, Kinetics of the β-AlFeSi to α-Al (FeMn) Si Transformation in Al-Mg-Si Alloys, doctoral thesis, TU Delft, 2004.

[58]. T. Sheppard, Extrusion of Aluminium Alloys, Springer Science & Business Media, 2013.

[59]. S. Liu, X. Wang, Q. Pan, M. Li, J. Ye, K. Li, Z. Peng, Y. Sun, Investigation of sitivity of Al–Mg–Si–Mn–Cr alloy during t, J. Alloys Compd. 826 (2020), 154144.

[60]. J.A. Österreicher, M. Kumar, A. Schiffl, S. Schwarz, G.R. Bourret, Secondary g-Si alloys: influence on high ess, Mater. Sci. Eng. A 687 (2017) 175–180.

[61]. A. R. Arnoldt et all., Influence of different homogenization heat treatments on the microstructure and hot flow stress of the aluminum alloy AA6082, Materials Characterization 191 (2022) 112129

[62]. Banhart J, Chang CSR, Liang Z, Wanderka N, Lay MDH, Hill AJ, et al. Natural aging in Al-Mg-Si alloys – A process of unexpected complexity. Adv. Eng. Mater 2010;12:559-571.

[63]. Mizuno K, Okamoto H, Hashimoto E, Kino T. Reduction of large vacancy clusters in nearly perfect aluminum single crystals. Trans. Mat. Res. Soc. Jpn 2016;41:243-246.

[64]. Hirsch PB, Silcox J, Smallman RE, Westmacott KH. Dislocation loops in quenched aluminium. Phil. Mag1958;3:897-908.

[65]. Yoshida S, Shimomura Y, Kiritani M. Dislocation loops containing a stacking fault in quenched superpurealuminum. J. Phys. Soc. Jpn 1962;17:1196.

[66]. Gavini V, Bhattacharya K, Ortiz M. Vacancy clustering and prismatic dislocation loop formation in aluminum. Phys. Rev. B 2007;76:180101.

[67]. Marioara CD, Nordmark H, Andersen SJ, Holmestad R. Post-beta'' phases and their influence on microstructure and hardness in 6xxx Al-Mg-Si alloys. Journal of Materials Science 2006;41:471-478.

[68]. Edwards GA, Stiller K, Dunlop GL, Couper MJ. The precipitation sequence in Al–Mg–Si alloys. Acta Mater 1998;46:3893-3904.

[69]. M. Baruah and A. Borah, Processing and precipitation strengthening of 6xxx series aluminium alloys: A review, International Journal of Materials Science 2020; 1(1): 40-48

[70]. Lynch JP, Brown LM, Jacobs MH. Microanalysis of age-hardening precipitates in aluminium alloys. Acta Metallurgica 1982;30:1389-1395.

[71]. Jacobs M. The structure of the metastable precipitates formed during ageing of an Al-Mg-Si alloy. Philosophical Magazine 1972;26:1-3.

[72]. Sekhar AP, Nandy S, Ray KK, Das D. Prediction of aging kinetics and yield strength of 6063. Journal of Materials Engineering and Performance 2019;28:2764-2778.

[73]. D. Chakrabarti, D. E. Laughlin, Prog. Mater. Sci. 2004, 49, 389.

[74]. C. D. Marioara, S. J. Andersen, T. N. Stene, H. Hasting, J. Walmsley, A. T. J. Van Helvoort, R. Holmestad, Philos. Mag. 2007, 87, 3385.

[75]. C. D. Marioara, et all., Metall. Mater. Trans. A 2014, 45, 2938.

[76]. M. Torsæter, F. J. H. Ehlers, C. D. Marioara, S. J. Andersen, R. Holmestad, Philos. Mag. 2012, 92, 3833.

[77]. C. Cayron, L. Sagalowicz, O. Beffort, P. A. Buffat, Philos. Mag. A 1999, 79, 2833.

[78]. T. Saito et,all., Atomic Structures of Precipitates in Al–Mg–Si Alloys with Small Additions of Other Elements, Adv. Eng. Mater. 2018, 1800125.

[79]. J.D. Robson et all., Advances in Microstructural Understanding of Wrought Aluminum Alloys, Metallurgical and Materials Transactions A, Volume 51A, September 2020—4377

[80]. H. Zhao, et all., Acta Mater., 2018, vol. 156, pp. 318–29.

[81]. Y.-Y. Li, L. Kovarik, P.J. Phillips, Y.-F. Hsu, W.-H. Wang, and M.J. Mills: Philos. Mag. Lett., 2012, vol. 92, pp. 166–78.

[82]. T. Marlaud, A. Deschamps, F. Bley, W. Lefebvre, and B. Baroux: Acta Mater., 2010, vol. 58, pp. 248–60.

[83]. A.R. Eivani et all., Evolution of Grain Boundary Phases during the Homogenization of AA7020 Aluminum Alloy, Metallurgicaland Materials Transactions A, Volume 40A, March 2009—717 .

[84]. Liu, S.; Chen, B.; Li, C.; Dai, Y.; Deng, Y.; Zhang, X. Mechanism of low exfoliation corrosion resistance due to slow quenching in high strength aluminium alloy. Corros. Sci. 2015, 91, 203–212.

[85]. Chen, S.-Y.; Chen, K.-H.; Peng, G.-S.; Liang, X.; Chen, X.-H. Effect of quenching rate on microstructure and stress corrosion cracking of 7085 aluminum alloy. Trans. Nonferrous Met. Soc. China 2012, 22, 47–52.

[86]. Kang, L.; Zhao, G.;Wang, G.-D.; Liu, K.; Tian, N. Effect of different quenching processes following solid-solution treatment on properties and precipitation behaviors of 7050 alloy. Trans. Nonferrous Met. Soc. China 2018, 28, 2162–2172

[87]. Song, F.X.; Zhang, X.M.; Liu, S.D.; Tan, Q.; Li, D.F. Exfoliation corrosion behavior of 7050-T6 aluminum alloy treated with various quench transfer time. Trans. Nonferrous Met. Soc. China 2014, 24, 2258–2265.

[88]. N. Jaburek, M. Merklein, Influence of a regression heat treatment on the material properties of a copper-free 7xxx series aluminum alloy, Procedia CIRP 18 (2014) 108 -113.

[89]. S. Jain, M.L.C. Lim, J.L. Hudson, J.R. Scully, Spreading of intergranular corrosion on the surface of sensitized Al-4.4Mg alloys: a general finding, Corros. Sci. 59 (2012) 136 -147.

[90]. J.G. Brunner, N. Birbilis, K.D. Ralston, S. Virtanen, Impact of ultrafine-grained microstructure on the corrosion of aluminium alloy AA2024, Corros. Sci. 57 (2012) 209 -214.

[91]. F.X. Song, X.M. Zhang, S.D. Liu, Q. Tan, D.F. Li, The effect of quench rate and overageing temper on the corrosion behaviour of AA7050, Corros. Sci. 78 (2014) 276- 286.

[92]. F.X. Song, X.M. Zhang, S.D. Liu, Q. Tan, The effect of quench transfer time on microstructure and localized corrosion behavior of 7050-T6 Al alloy, Mater. Corros. 65 (2014) 1007-1016.

[93]. K.A. Unocic, P. Kobe, M.J. Mills, G.S. Daehn, Grain boundary precipitate modification for improved intergranular corrosion resistance, Mater. Sci. Forum 519e521 (2006) 327 - 332.

[94]. A.S. Elamoush, Intergranular corrosion behavior of the 7075-T6 aluminum alloy under different annealing conditions, Mater. Chem. Phys. 126 (2011) 607- 613.

[95]. D.K. Xu, N. Birbilis, D. Lashansky, P.A. Rometsch, B.C. Muddle, Effect of solution treatment on the corrosion behaviour of aluminium alloy AA7150: optimization for corrosion resistance, Corros. Sci. 53 (2011) 217 -225.

[96]. J.F. Chen, G.S. Frankel, J.T. Jiang, W.Z. Shao, L. Zhen, Effect of age-forming on corrosion properties of an Al-Zn-Mg-Cu alloy, Mater. Corros. 65 (2014) 670 - 677.

[97]. A. Khalfallah, A. Raho, S. Amzert, A. Djemli, Precipitation kinetics of GP zones, metastable η′ phase and equilibrium η phase in Al-5.46wt%Zn-1.67wt%Mg alloy, Trans. Nonferrous Met. Soc. China 29 (2) (2019) 233–241.

[98]. Y.S. Lee, D.H. Koh, H.W. Kim, Y.S. Ahn, Improved bake-hardening response of Al–Zn–Mg–Cu alloy through pre-aging treatment, Scr. Mater. 147 (2018) 45–49.

[99]. J.Z. Liu, J.H. Chen, X.B. Yang, S. Ren, C.L. Wu, H.Y. Xu, J. Zou, Revisiting the precipitation sequence in Al–Zn–Mg-based alloys by high-resolution transmission electron microscopy, Scr. Mater. 63 (11) (2010) 1061–1064.

[100]. L.K. Berg, J. Gjonnes, V. Hansen, X.Z. Li, M. Knutson-Wedel, G. Waterloo, D. Schryvers, L.R. Wallenberg, GP-zones in Al–Zn–Mg alloys and their role in artificial aging, Acta Mater. 49 (17) (2001) 3443–3451.

[101]. G. Sha, A. Cerezo, Early-stage precipitation in Al–Zn–Mg–Cu alloy (7050), Acta Mater. 52 (15) (2004) 4503–4516.

[102]. J. Chen, L. Zhen, S. Yang, W. Shao, S. Dai, Investigation of precipitation behavior and related hardening in AA 7055 aluminum alloy, Mater. Sci. Eng. A 500 (1–2) (2009) 34–42.

[103]. M. Liu, B. Klobes, K. Maier, On the age-hardening of an Al–Zn–Mg–Cu alloy: a vacancy perspective, Scr. Mater. 64 (1) (2011) 21–24.

[104]. Z. Chen Zhongwei Chen et all., Precipitation sequence and hardening effect in 7A85 aluminum alloy Precipitation sequence and hardening effect in 7A85 aluminum alloy, Journal of Alloys and Compounds 875 (2021) 159950

[105]. K. Wen, Y. Fan, G. Wang, L. Jin, X. Li, Z. Li, Y. Zhang, Aging behavior and precipitate characterization of a high Zn-containing Al–Zn–Mg–Cu alloy with various tempers, Mater. Des. 101 (2016) 16–23.

[106]. T.F. Chung, Y.L. Yang, B.M. Huang, Z. Shi, J. Lin, T. Ohmura, J.R. Yang, Transmission electron microscopy investigation of separated nucleation and in-situ nucleation in AA7050 aluminium alloy, Acta Mater. 149 (2018) 377–387.

[107]. T.F. Chung, Y.L. Yang, M. Shiojiri, C.N. Hsiao, W.C. Li, C.S. Tsao, Z. Shi, J. Lin, J.R. Yang, An atomic scale structural investigation of nanometre-sized η precipitates in the 7050 aluminium alloy, Acta Mater. 174 (2019) 351–368.

[108]. K. Wen, Y. Fan, G. Wang, L. Jin, X. Li, Z. Li, Y. Zhang, Aging behavior and precipitate characterization of a high Zn-containing Al–Zn–Mg–Cu alloy with various tempers, Mater. Des. 101 (2016) 16–23.

[109]. S. Lee, D.H. Koh, H.W. Kim, Y.S. Ahn, Improved bake-hardening response of Al–Zn–Mg–Cu alloy through pre-aging treatment, Scr. Mater. 147 (2018) 45–49.

[110]. J.Z. Liu, J.H. Chen, X.B. Yang, S. Ren, C.L. Wu, H.Y. Xu, J. Zou, Revisiting the precipitation sequence in Al–Zn–Mg-based alloys by high-resolution transmission electron microscopy, Scr. Mater. 63 (11) (2010) 1061–1064.

[111]. L.K. Berg, J. Gjonnes, V. Hansen, X.Z. Li, M. Knutson-Wedel, G. Waterloo, D. Schryvers, L.R. Wallenberg, GP-zones in Al–Zn–Mg alloys and their role in artificial aging, Acta Mater. 49 (17) (2001) 3443–3451.

[112]. G. Sha, A. Cerezo, Early-stage precipitation in Al–Zn–Mg–Cu alloy (7050), Acta Mater. 52 (15) (2004) 4503–4516.

[113]. J.Chen, L. Zhen, S. Yang, W. Shao, S. Dai, Investigation of precipitation behavior and related hardening in AA 7055 aluminum alloy, Mater. Sci. Eng. A 500 (1–2) (2009) 34–42.

[114]. G. Shaand A. Cerezo., Characterization of precipitates in an aged 7xxx series Al alloy, Surf. Interface Anal. 2004; 36: 564–568

[115]. Y. Hu, G. Wang, W. Wang, Y. Rong, Effect of precipitation during quenching on the prediction of the mechanical properties of Al-5 Pct Cu alloy after T6 treatment, Metall. Mater. Trans. A Phys. Metall. Mater. Sci. 48 (2017) 5667–5677.

[116]. M. Zhang, W. Zhang, H. Zhao, D. Zhang, Y. Li, Effect of pressure on microstructures and mechanical properties of Al-Cu-based alloy prepared by squeeze casting, Trans. Nonferrous Metals Soc. China 17 (2007) 496–501.

[117]. M. Tiryakioğlu, R.T. Shuey, Quench sensitivity of 2219-T87 aluminum alloy plate, Mater. Sci. Eng. A 527 (2010) 5033–5037.

[118]. X. Zhang, B. Liu, X. Zhou, J. Wang, T. Hashimoto, C. Luo, Z. Sun, Z. Tang, F. Lu, Laser welding introduced segregation and its influence on the corrosion behaviour of Al-Cu-Li alloy, Corros. Sci. 135 (2018) 177–191.

[119]. R. Guo, J.Wu, Dislocation densitybased model for Al-Cu-Mg alloy during quenching with considering the quench-induced precipitates, J.Alloys Compd. 741 (2018) 432–441.

[120]. Y. Yin, B. Luo, H. Jing, Z. Bai, Y. Gao, Influences of quench cooling rate on microstructure and corrosion resistance of Al-Cu-Mg alloy based on the end-quenching test, Metall. Mater. Trans. B 49 (2018) 2241–2251.

[121]. S. Luo, G. Wang, Y. Hu, Y. Zhong, Y. Rong, Effect of quenching rate and its coupling model on precipitation and strength of Al–Cu–Cd alloys, Mater. Sci. Eng. A 761 (2019) 138022.

[122]. ASKELAND, Donald. (1998). Ciencia e ingeniería de los materiales. En Ensayos y propiedades mecánicas (págs. 143-146). México : International Thomson

[123]. D.A. Porter, K.E. Easterling, M. Sherif, Phase Transformations in Metals and Alloys, third ed., CRC Press, 2009.

[124]. S.C. Wang, M.J. Starink, Precipitates and intermetallic phases in precipitation hardening Al-Cu-Mg(Li) based alloys, Int. Mater. Rev. 50 (2005) 193-215.

[125]. I. .Zuiko and R. Kaibyshev., Aging behavior of an Al- Cu-Mg alloy, Journal of Alloys and Compounds 759 (2018) 108-119

[126]. I.S. Zuiko, M.R. Gazizov, R.O. Kaibyshev, Effect of thermomechanical treatment on the . microstructure, phase composition, and mechanical properties of AleCueMneMgeZr alloy, Phys.

[127]. Met. Metallogr 117 (2016) 906-919.

[128]. L. Ye, G. Gu, J. Liu, H. Jiang, X. Zhang, Influence of Ce addition on impact properties and microstructures of 2519A aluminum alloy, Mater. Sci. Eng. A 582 (2013) 84-90.

[129]. L. Ye, G. Gu, X. Zhang, D. Sun, H. Jiang, P. Zhang, Dynamic properties evaluation of 2519A aluminum alloy processed by interrupted aging, Mater. Sci. Eng. A 590 (2014) 97-100.

[130]. Zh. Xin-ming et all., Effects of Yb addition on microstructures and mechanical properties of 2519A aluminum alloy plate, Trans. Nonferrous Metals Soc. China 20 (2010) 727-731.

[131]. J.Z. Liu, S.S. Yang, S.B. Wang, J.H. Chen, C.L. Wu, The influence of Cu/Mg atomic ratios on precipitation scenarios and mechanical properties of Al-Cu-Mg alloys, J. Alloys Compd. 613 (2014) 139- 142.

[132]. Z. Gao, X. Zhang, M. Chen, Investigation on θ′ precipitate thickening in 2519A- T87 aluminum alloy plate impacted, J. Alloys Compd. 476 (2009) L_1-L_3.

[133]. Wen-tao Wang, Xin-ming Zhang, Zhi-guo Gao, Yu-zhen Jia, Ling-ying Ye, Da- wei Zheng, Ling Liu, Influences of Ce addition on the microstructures and mechanical properties of 2519A aluminum alloy plate, J. Alloys Compd. 491 (2010) 366-371.

[134]. S.P. Ringer, B.T. Sofyan, K.S. Prasad, G.C. Quan, Precipitation reactions in Al-4.0Cu-0.3Mg (wt.%) alloy, Acta Mater. 56 (2008) 2147-2160.

[135]. M. Gazizov, R. Kaibyshev, Precipitation structure and strengthening mechanisms in an Al- Cu-Mg- Ag alloy, Mater. Sci. Eng. A 702 (2017) 29 - 40.

[136]. F.J. Nie, B.C. Muddle, Microstructural design of high strength aluminum alloys, J. Phase Equil. 19 (6) (1998) 543 - 551.

[137]. B. Zlaticanin, S. Duric, B. Jordovic and B. Radonjic, Comunications Ltd. Published by maney for the Institute of Metrials, Minerals and Mining, pp. 10-15, 2003.

[138]. Y.A. Bagaryatskii: Dokl. Akad. Nauk SSSR, 1952, vol. 87, pp. 397–400.

[139]. Y.A. Bagaryatskii: Dokl. Akad. Nauk SSSR, 1952, vol. 87, pp. 559–61.

[140]. J.M. Silcock: J. Inst. Met., 1960–61, vol. 89, pp. 203–10.

[141]. H. Perlitz and A. Westgren: Arkiv Kemi Mineral. Geol., 1943, vol. 16B (13), pp. 990–94.

[142]. A. Charai, T. Walther, C. Alfonso, A.-M. Zahra, and C.Y. Zahra: Acta Mater., 2000, vol. 48, pp. 2751–64.

[143]. T. Takahashi and T. Sato: Keikinzoku, 1985, vol. 35 (1), pp. 41–49.

[144]. L. Kovarik, P. Gouma, C. Kisielowski, S.A. Court, and M.J. Mills: Acta Mater., 2004, vol. 52, pp. 2509–20.

[145]. H.-C. Shih, N.-J. Ho, and J.C. Huang: Metall. Mater. Trans. A, 1996, vol. 27A, pp. 2479–94.

[146]. S.C. Wang, M.J. Starink, and N. Gao: Scripta Mater., 2006, vol. 54, pp. 287–91.

[147]. H. LU et all., Precipitation Behavior of AA2618, Metallurgical and Mmaterials TransactionsA, Volume 38A, October 2007—2379

[148]. H. I. Aaronson, Mechanisms of Phase Transformations in Crystalline Solids, Institute of Metals,

[149]. T.J.Bastow and A.J.Hill., Guinier-Preston and Guinier-Preston-Bagaryatsky zone reversion in Al-Cu-Mg alloys studied by NMR, Materials Science Forum Vols. 519-521 (2006) pp 1385-1390

[150]. D. Porter, and K. Easterling: Phase Transformations in Metals and Alloys, 2nd edition, (London; New York: Chapman and Hall 1992).

[151]. L. Kovarik, PI. Gouma, C. Kisielowski, S.A. Court and M. J. Mills, Acta mater, Vol 52 (2004) p. 2509

[152]. J. Majimel, G. Molenat, F. Danoix, O. Thuillier, D. Blavette, G. Lapasset, and M.- J. Casanove, Phil. Mag., Vol 84 (2004) p. 3263.

[153]. T.J.Bastow, Phil Mag, Phil. Mag., Vol 85 (2005) p. 1053.London, U.K., 1969, p. 270.

[154]. Nicholson, R.B. and Nutting, J., Acta Metall., 9, 332, 1961.

[155]. Bagaryatsky YA. Doklady Akademii SSSR 1952;87:397.

[156]. Bagaryatsky YA. Doklady Akademii SSSR 1952;87:559.

[157]. Silcock JM. J Inst Metals 1960-61;89:203.

[158]. L. Kovarik et all., GPB zones and composite GPB/GPBII zones in Al–Cu–Mg alloys, Acta Materialia 56 (2008) 4804–4815